

DESIGN AND EXPERIMENTAL STUDY OF CLEANING DEVICE FOR WHEAT HARVESTER BASED ON CFD-DEM

基于 CFD-DEM 的制繁种小麦收获机清选装置的设计与试验研究

Ranbing YANG^{1,2}, Shuai WANG¹, Zhiguo PAN¹, Guoying LI³, Yalong SHU¹,
Qi LIU¹, Zhen LIU¹, Yihui MIAO¹

¹ College of Electrical and Mechanical Engineering, Qingdao Agricultural University, Qingdao/ China

² College of Mechanical and Electrical Engineering, Hainan University, Haikou/ China

³ Qingdao Pulantech Machinery Technology Co., Ltd., Qingdao/ China

Tel: +8615318715305; E-mail: peter_panzg@163.com

Corresponding author: Zhiguo Pan

DOI: <https://doi.org/10.35633/inmateh-75-49>

Keywords: Wheat harvester, Seed production and propagation, Cleaning device, Coupled simulation

ABSTRACT

To address the issues of high admixture and loss rates during seed production and harvesting operations with combine harvesters, a low-loss, high-purity cleaning device suitable for wheat seed production and harvesting was designed. Considering the actual conditions of seed production and harvesting operations, the structure and dimensional parameters of key components were optimized. Through theoretical analysis, a motion model of wheat seeds on the cleaning sieve was established, identifying the main factors affecting the cleaning performance as fan speed, sieve amplitude, and vibration frequency. The CFD-DEM coupling method was used to simulate and analyze the sieving process under the influence of airflow within the cleaning chamber. A three-factor, three-level quadratic regression orthogonal combination simulation test was conducted to establish a response surface regression model for the seed admixture rate and the seed loss rate. Multi-objective comprehensive optimization of the factors indicated that the optimal operating parameters of the cleaning device are a fan speed of 1143 rpm an amplitude of 28 mm, and a vibration frequency of 9.4 Hz. Finally, field trial verification was conducted by setting the working parameters based on the coupled simulation test data. The operational results of the optimized cleaning device showed a seed admixture rate of 1.47% and a seed loss rate of 1.07%, with all results meeting the relevant standards. This study can provide valuable theoretical support for the development of wheat seed production and harvesting machines.

摘要

为解决联合收获机在进行制繁种收获作业时混杂率、损失率较高等问题，设计了一款适用于小麦制繁种收获作业的低损高净度清选装置。结合实际制繁种收获作业情况，优化了关键部件的结构及尺寸参数。通过理论分析，建立了小麦种子在清选筛上的运动模型，确定了影响清选效果的主要因素为风机转速、清选筛振幅和振动频率。采用 CFD-DEM 耦合方法对清选室内部气流作用下的筛分过程进行模拟分析，开展了三因素三水平二次回归正交组合仿真试验，建立了种子混杂率和种子损失率的响应面回归模型，对各因素进行多目标综合优化，结果表明：风机转速 1143 rpm、振幅 28 mm、振动频率 9.4 Hz，是清选装置的最优工作参数。最后，以耦合仿真试验数据为基础设置工作参数，进行田间试验验证，优化后的清选装置作业结果为：种子混杂率 1.47 %、种子损失率 1.07 %，结果各项均满足相关标准。本研究可为小麦制繁种收获机的研发提供有价值的理论依据。

INTRODUCTION

Seed multiplication, as a sophisticated integration of breeding technology and propagation techniques, plays an indispensable strategic role in meeting the urgent demands of agricultural production by cultivating high-quality, high-yield seeds. It significantly contributes to enhancing agricultural productivity, ensuring food security, promoting green development, and fostering economic prosperity, thus exerting a profound impact on the sustainable development of global agriculture (Mehta et al., 2019; Török et al., 2019; Krishna et al., 2023).

However, there is currently a severe scarcity of intelligent operational equipment specifically designed for seed multiplication harvesting. This deficiency directly affects the cost and efficiency of seed production, becoming a bottleneck that hinders the rapid development of the seed industry. Compared to field crop harvesting, seed multiplication harvesting faces more complex challenges: factors such as the diversity of

experimental varieties and the close proximity between adjacent seed plots make the process arduous (Lalghorbani *et al.*, 2022; Parihar *et al.*, 2023; Cheli *et al.*, 2024). At present, there is no dedicated machine type for wheat seed multiplication harvesting, and combine harvesters are typically used as substitutes. Although the mechanized operation technology in the wheat industry has matured, it still struggles to meet the stringent requirements of seed multiplication regarding key technical indicators such as loss rate, seed damage rate, and breakage rate, necessitating further optimization and enhancement at critical mechanisms and technical levels.

Delaney *et al.*, (2012), employed the EDEM method to study the impact of particle models on sieving motion, discovering that using single spherical particles in sieving motion simulations is insufficient to accurately simulate the actual flow and separation of non-spherical particles.

Ivan *et al.*, (2015), investigated factors influencing threshing capacity in conventional grain combine harvesters, providing a theoretical foundation for enhancing operational efficiency.

Buryanov *et al.*, (2019), designed a threshing device with adjustable concave spacing, effectively reducing loads on blowers and cleaning sieves.

Hevko *et al.*, (2019), established a mathematical model for the cleaning and conveying system of root/tuber crops, offering theoretical guidance for cleaner design.

Safranyik *et al.*, (2019), investigated the movement patterns of spherical particles during the cleaning process and determined the optimal operating parameters of the cleaning sieve using analytical methods, while also employing DEM to analyze the impact of interactions among multiple particles moving on the sieve surface.

Mircea *et al.*, (2020), developed an internal helical coil to optimize cyclone separator performance in cleaning systems.

Vlăduț *et al.*, (2022), proposed a mathematical model describing threshing-separation processes in axial-flow threshers, establishing theoretical principles for device design and optimization.

Vlăduț *et al.*, (2023), determined optimal operating parameters for cleaning-threshing systems during harvesting by analyzing key influencing factors.

Marin *et al.*, (2023), evaluated the impact of primary vibration sources in grain harvesters on operators, delivering theoretical insights for machine design refinement.

Wang *et al.*, (2024), adopted a CFD-DEM coupling approach to simulate operations under different field conditions, analyzing how various design parameters affect operational outcomes. They then validated their findings through experiments, thereby determining the optimal design scheme for a new type of wheat harvester.

This paper is based on the study of grain combine harvesters and addresses the issues of high seed contamination and loss rates during seed multiplication operations. It proposes a cleaning device specifically suitable for seed multiplication harvesting. Through an integrated method combining coupled simulation and field experiments, the key structures and parameters of the cleaning device are optimized, aiming to provide valuable insights for the research of cleaning devices in wheat seed multiplication harvesters.

MATERIAL AND METHODS

OVERALL STRUCTURE DESIGN OF THE CLEANING DEVICE

The use of conventional grain combine harvester cleaning devices results in a high residue of seeds, which easily leads to the mixing of different seed varieties, making it difficult to meet the requirements for seed multiplication. Traditional centrifugal fans tend to cause material accumulation in front of the sieve area, and when the wind speed is high, the loss rate increases; conversely, when the wind speed is low, the residue amount is substantial. To enhance cleaning efficiency and achieve the expected targets for seed multiplication harvesting, a cleaning device suitable for wheat seed multiplication harvesting has been designed, as shown in the figure 1.

The main functional components of the cleaning device include a centrifugal fan, cleaning sieve, shaking plate, and auger. During operation, the wheat threshed mixture falls through the concave sieve of the drum onto the shaking plate and cleaning sieve. Under the impetus of the centrifugal fan, the material becomes fluidized. Light impurities such as bran and short stalks are directly expelled from the cleaning chamber by the fan. Stalks are discharged from the debris outlet through the reciprocating motion of the fan and cleaning sieve. The wheat grains fall into the grain collection auger, while a small portion of the inadequately cleaned threshed mixture undergoes secondary cleaning through the debris auger.

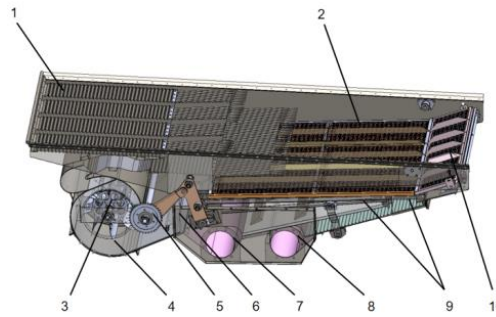


Fig. 1 – Overall structure of the cleaning device
 1. Shaking plate; 2. Cleaning sieve; 3. Fan impeller; 4. Fan volute; 5. Wind guide plate; 6. Eccentric rod gear;
 7. Grain-gathering dragon; 8. Miscellaneous dragon; 9. Baffle; 10. Tail sieve

DESIGN OF KEY COMPONENTS OF THE CLEANING DEVICE

Design of Dual Air Duct Centrifugal Fan

As the core component of the pneumatic conveying system, the performance of the fan affects the operational efficiency of the machine. Most grain combine harvesters use single-outlet centrifugal fans, which are characterized by simple structure, easy installation, and high wind pressure, performing well in high-resistance environments. However, existing research indicates that during wheat mechanical harvesting, the threshed mixture is unevenly distributed on the sieve surface, exhibiting a “V” shape with thicker material at the front and thinner at the back, as well as more material on the sides than in the center (Li et al., 2012; Fu et al., 2024) This suggests that the airflow of single-outlet centrifugal fans has coverage blind spots, making it difficult to cover the entire sieve surface, which is unfavorable for cleaning operations. Therefore, it is necessary to design a centrifugal fan suitable for seed breeding harvesting, taking into account the characteristics of seed breeding harvesting and the distribution pattern of the wheat threshed mixture, to achieve the desired objectives.

Design of Radial Dual-Fan Impeller

The impeller is the core component of a centrifugal fan, and its rotation drives the airflow throughout the cleaning chamber. Therefore, its structural and dimensional parameters have a decisive impact on the performance of the fan. Impellers can be classified into forward, radial, and backward types based on the blade exit angle. To meet the operational requirements of seed breeding harvesting, a radial blade dual-fan impeller has been designed. The main design parameters of the impeller include the outer diameter D_1 , inner diameter D_2 , blade length B , blade thickness t , and the number of blades. The structure and main parameters of the fan impeller are shown in the figure 2.

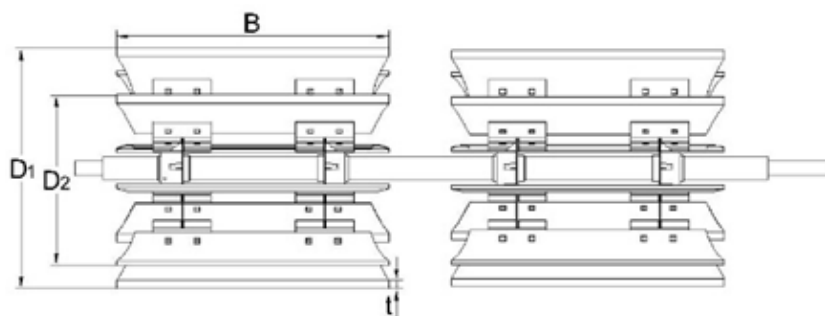


Fig. 2 – Fan Impeller Mode

Table 1

Fan Impeller Structural Parameters	
Parameter	Numerical value
Impeller diameter D_1 (mm)	400
Inner diameter of impeller D_2 (mm)	288
Blade length B (mm)	470
Blade thickness t (mm)	2
Blade quantity	8

Design of Blade Airfoil

The seed breeding and harvesting process is characterized by “tight schedules, heavy tasks, and high demands.” The fan in the cleaning system, which is responsible for sorting the mixture after threshing, must maintain stable operation for extended periods during the seed breeding and harvesting season. However, traditional straight blade designs often lead to unstable airflow separation and additional energy loss, directly resulting in decreased fan efficiency. To address this challenge, it is necessary to improve and upgrade the structural parameters of the fan blades (Zhang *et al.*, 2023). First, the blade bending angle should be adjusted. By utilizing fluid dynamics simulations and digital calculations, the optimal blade bending angle can be identified to ensure that airflow adheres more closely to the blade contour, thereby reducing flow separation and turbulence losses. Secondly, the leading edge of the blade has been modified to have a blunt angle. By optimizing the width ratio of the blade’s leading edge, pressure concentration is improved, and by adjusting the curvature of the blade’s leading edge to form a longer contraction passage, the range of efficient operating conditions for the blade is further expanded while ensuring stable operation under high-intensity conditions.

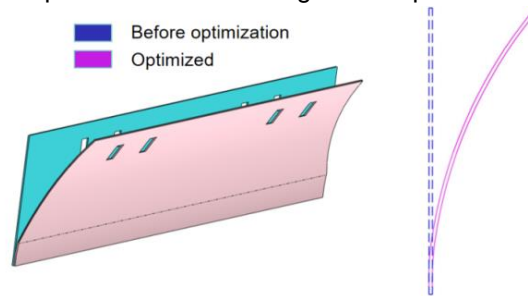


Fig. 3 – Comparison of Airfoil Before and After Optimization

Design of Fan Scroll Casing

The fan scroll casing serves the purpose of collecting and directing the accelerated airflow from the impeller, aiding in the circulation of airflow within the fan and converting part of the kinetic energy into static pressure energy. Due to the complex three-dimensional flow of gases inside a centrifugal fan, the scroll casing is filled with vortex structures of varying scales and intensities. Therefore, the scroll casing’s profile not only determines the guidance of airflow but also affects the flow loss within the fan, directly impacting the aerodynamic performance, output airflow, and pressure parameters of the entire fan. Currently, two widely used scroll profiles are the logarithmic spiral and the Archimedean spiral. The centrifugal fan scroll designed in this study is based on the Archimedean spiral, characterized by a smoothly curved equidistant spiral, which suppresses the formation of vortex regions within the scroll passage while maximizing airflow along the spiral. The main parameter calculations are shown in the table below, according to the Agricultural Machinery Design Manual:

Table 2

Fan Scroll Structural Parameters	
Parameter	Numerical value
Lower air outlet height L_1 (mm)	258
Upper air outlet height L_2 (mm)	84
Vertical distance H (mm)	186
Thread extension dimensions A	100
$R_1 = D_1/2 + (2/5)A$	240
$R_2 = D_1/2 + (9/10)A$	290
$R_3 = D_1/2 + (3/10)A$	230
$R_4 = D_1/2 + A/2$	250
$R_5 = D_1/2 + (4/5)A$	280

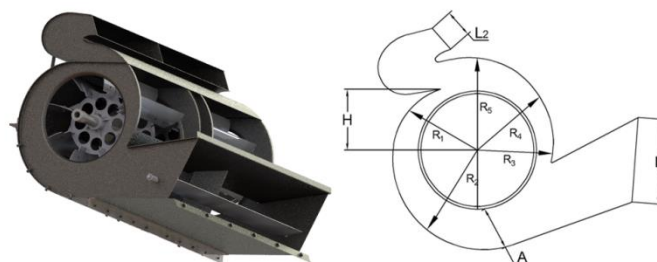


Fig. 4 – Fan Scroll Model

Design of Cleaning Sieve

As the core component of the cleaning device, the cleaning sieve plays a decisive role in the stratification and conveying movements of materials on the sieve surface. According to the shape and structure of the screen, cleaning sieves can be categorized into fish scale sieves, perforated sieves, bar sieves, etc. Among them, perforated sieves are mostly used for fine screening of small particles; bar sieves tend to experience hole blockage and beam fracture under high-intensity conditions; whereas fish scale sieves are composed of curved fish scale sieve plates with adjustable openings according to actual working conditions. They have a strong capability to convey residues without clogging easily, and the airflow on the sieve surface is uniform, which can meet the requirements of complex working conditions during seed production and harvesting.



Fig. 5 – Schematic Diagram of Cleaning Sieve

In cleaning operations, the mesh size is related to the feed rate. Referring to the "Agricultural Machinery Design Handbook," the formula for calculating the total length L of the sieve is:

$$L = \frac{F_z}{WF_s} \quad (1)$$

In the formula: F_z is the Machine feed rate; W is the Screen surface width; F_s is the feed rate that can be handled per unit area of the sieve.

Based on the actual feed rate and the actual grain quality on the sieve surface during the seed production and harvest process, the value of F_z is 4 kg/s, and the value of F_s is 2.4 kg/(s·m²). Considering the combination of the cleaning device with the frame and the single longitudinal axial flow drum threshing device, the sieve width is 1200 mm. Substituting these into the formula yields a value of L being 1390 mm. Taking into account that the mass of the material entering the cleaning device is approximately half of the drum's feed rate, the design of the cleaning sieve meets agronomic requirements.

Design of Eccentric Linkage Mechanism

The cleaning sieve achieves material stratification and movement towards the outlet through sieving motion. The specific motion process involves a deep groove ball bearing with an eccentric sleeve, which is positioned on the drive shaft using a shaft elastic retaining ring. The lower side of the connecting rod is fitted onto the deep groove ball bearing, while the upper side is hinged to the rocker arm with a bolt. The rocker arm is hinged to both the frame and the sieve base frame. A chain drive rotates the eccentric wheel at a constant angular velocity, and the connecting rod transmits this motion to the sieve frame, converting the rotational motion of the eccentric wheel into the reciprocating motion of the sieve frame. This motion pushes the material on the sieve surface towards the outlet and stratifies it. A schematic diagram of the structure is shown in the illustration.



Fig. 6 – Schematic Diagram of Eccentric Linkage Mechanism

Since the eccentric linkage mechanism is closed at both ends, it can be considered a closed-chain mechanism. Its degree of freedom analysis is as follows:

$$F = 3n - 2F_l - F_h \quad (2)$$

In the formula 2, F represents the degree of freedom of the mechanism; n represents the number of active components; F_l denotes the number of lower pairs; F_h represents the number of high pairs.

Analysis shows that there are 3 movable links, 4 lower pairs, and 0 higher pairs in this crank-link mechanism. Therefore, the degree of freedom is calculated as 1, meaning that only one input of power is required to enable the vibrating screen to achieve reciprocating motion.

MOTION ANALYSIS OF WHEAT SEEDS ON THE CLEANING SCREEN

After wheat seeds leave the shaking plate and enter the cleaning device, they move in the form of individual free particles. Therefore, when analyzing their forces in the airflow field, the focus should be on the individual behavior of wheat seed particles. When these particles fall onto the cleaning screen, the screen undergoes reciprocating motion, also known as simple harmonic motion, driven by a crank-rocker mechanism. During this process, the movement of materials on the screen surface primarily exhibits three states: forward sliding, backward sliding, and throwing. These movement states significantly affect the screening effect and separation efficiency of wheat from mixtures. Therefore, these motion characteristics must be fully considered in the design and optimization of cleaning devices.

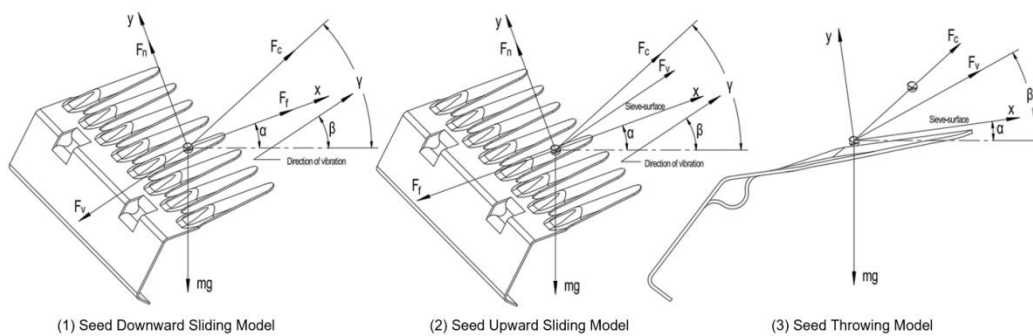


Fig. 8 – Analysis of Seed Motion States on the Cleaning Screen

Analysis of Seed Sliding Down the Screen Surface

According to D'Alembert's principle, when seeds are considered as rigid bodies and their motion on the screen surface is taken into account, a dynamic problem can be transformed into a static problem. By introducing inertial force, the main forces, constraint forces, and inertial forces of the particles formally constitute a system of equilibrium forces. In this context, a sliding motion model for the seeds can be established. When the seeds slide down the screen surface under the action of their inertial force and the direction of acceleration is positive, the motion model of the seeds can be described as follows:

$$F_c \sin(\gamma - \alpha) + F_n = mg \cos \alpha + F_v \sin(\beta - \alpha) \tag{3}$$

$$F_c \cos(\gamma - \alpha) + F_f = mg \sin \alpha + F_v \cos(\beta - \alpha) \tag{4}$$

In the formula, F_v denotes the inertial force; F_f denotes friction; F_c represents the wind power of the fan; α represents the inclination of the screen surface; β represents the vibration direction angle; γ indicates the airflow direction angle; φ denotes the friction angle.

Substituting the relevant parameters and performing rearrangement and simplification, the following is obtained:

$$\frac{\omega^2 r}{g} \cos \omega t = \left(\frac{V}{V_p}\right)^2 \cdot \frac{\cos(\gamma - \alpha + \varphi)}{\cos(\beta - \alpha + \varphi)} - \frac{\sin(\alpha - \varphi)}{\cos(\beta - \alpha + \varphi)} \tag{5}$$

In which, $\cos \omega t \leq 1$. The critical condition for the seeds to slide down the screen surface is:

$$\frac{\omega^2 r}{g} > \left(\frac{V}{V_p}\right)^2 \cdot \frac{\cos(\gamma - \alpha + \varphi)}{\cos(\beta - \alpha + \varphi)} - \frac{\sin(\alpha - \varphi)}{\cos(\beta - \alpha + \varphi)} \tag{6}$$

Analysis of Seed Sliding Up the Screen Surface

Similarly, when the seeds slide up the screen surface under the action of their own inertial force and the direction of acceleration is negative, the motion model of the seeds can be described as:

$$F_v \cos(\beta - \alpha) + F_c \cos(\gamma - \alpha) = F_f + mg \sin \alpha \tag{7}$$

$$F_n + F_c \sin(\gamma - \alpha) + F_v \sin(\beta - \alpha) = mg \cos \alpha \quad (8)$$

Substituting the relevant parameters and performing rearrangement and simplification, the following is obtained:

$$\frac{\omega^2 r}{g} \cos \omega t = \frac{\sin(\alpha + \varphi)}{\cos(\beta - \alpha - \varphi)} - \left(\frac{V}{V_p} \right)^2 \cdot \frac{\cos(\gamma - \alpha - \varphi)}{\cos(\beta - \alpha - \varphi)} \quad (9)$$

In which, $\cos \omega t \leq 1$. The critical condition for the seeds to slide up the screen surface is:

$$\frac{\omega^2 r}{g} > \frac{\sin(\alpha + \varphi)}{\cos(\beta - \alpha - \varphi)} - \left(\frac{V}{V_p} \right)^2 \cdot \frac{\cos(\gamma - \alpha - \varphi)}{\cos(\beta - \alpha - \varphi)} \quad (10)$$

Analysis of Seed Detachment from the Screen Surface

Analyzing the forces acting on seeds on the cleaning screen, it is evident that when the inertial force F_v is positive, and as the centripetal acceleration $\omega^2 r$ continuously increases, the support force F_n from the cleaning screen on the seeds decreases, gradually approaching zero.

At this point, the seeds, propelled by their own inertial force and the wind force from the cleaning fan, tend to be thrown off the surface of the cleaning screen. When the support force F_n exerted by the cleaning screen on the seeds equals zero, the seeds detach from the screen surface. Simultaneously, at the moment when the seeds begin to detach, sliding no longer occurs on the screen teeth, and the friction force disappears. At this moment, the motion model of the seeds can be described as:

$$F_N = mg \cos \alpha - F_v \sin(\beta - \alpha) - F_c \sin(\gamma - \alpha) \quad (11)$$

Substituting the relevant parameters and performing rearrangement and simplification, the following is obtained:

$$\frac{\omega^2 r}{g} \cos \omega t = \frac{\cos \alpha}{\sin(\beta - \alpha)} - \left(\frac{V}{V_p} \right)^2 \frac{\sin(r - \alpha)}{\sin(\beta - \alpha)} \quad (12)$$

In which, $\cos \omega t \leq 1$. The critical condition for the seeds to detach from the screen surface is:

$$\frac{\omega^2 r}{g} \geq \frac{\cos \alpha}{\sin(\beta - \alpha)} - \left(\frac{V}{V_p} \right)^2 \frac{\sin(r - \alpha)}{\sin(\beta - \alpha)} \quad (13)$$

In summary, the motion state of wheat seeds on the cleaning screen, apart from their own factors, is jointly determined by the airflow velocity and the acceleration ratio of the cleaning screen's motion (i.e., the fan speed and the vibration amplitude and frequency of the cleaning screen). To ensure cleaning performance, it is generally required that seeds can slide up and down on the screen surface while minimizing the occurrence of detachment from the screen. Therefore, finding the optimal combination of fan speed, amplitude, and vibration frequency is crucial for achieving good cleaning results. Due to the relatively complex motion patterns during the actual seed propagation and harvesting process, it is impossible to obtain accurate and effective dynamic data. Conducting numerical simulations of the airflow field in the cleaning chamber without material particles or vibration screening without airflow alone is incomplete. Therefore, it is necessary to use the coupled FLUENT and EDEM method, known as the CFD-DEM approach, to determine the optimal parameter range and combinations for key factors such as amplitude, airflow velocity, and airflow direction angle (Ding et al., 2022; Li et al., 2022).

RESULTS

RESEARCH ON THE MATERIAL MOVEMENT PATTERNS IN CLEANING DEVICES BASED ON CFD-DEM

To facilitate subsequent analysis, simulation models of the cleaning screen and the wheat threshing mixture were constructed using SOLIDWORKS and EDEM software. Orthogonal experiments were conducted with the seed impurity rate and seed loss rate as the main evaluation indicators, laying the foundation for further field trials and optimization of parameter combinations.

CFD Model of Cleaning Device

Firstly, considering the workload of coupled simulations and the computational capacity of the computer, a simplified 3D model of the cleaning chamber was constructed using SOLIDWORKS. Subsequently, the model in .STEP format from SOLIDWORKS was converted into a fluid domain model in .IGES format, which is recognizable by FLUENT, for meshing. The mesh was divided using a multi-module partitioning method, with the element size set between 0-1000 mm depending on the density. The total number of mesh elements was 45,422,210. The model after meshing is shown in the figure.

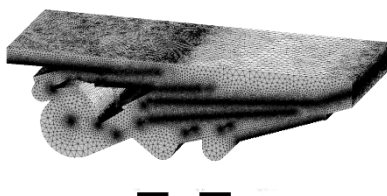


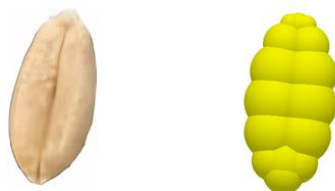
Fig. 9 – Schematic diagram of the cleaning room meshing

Then, the boundary conditions were set: both outlets of the centrifugal fan were assigned velocity-inlet boundary conditions, while the outlet was set as a pressure-outlet boundary. The fan impeller was configured with rotor-wall conditions, and the remaining areas were set as wall conditions. The k-epsilon model was chosen for the computational model, with the Standard Wall Function selected for the wall functions. The solution method employed was coupled, and the time step in FLUENT was set to 0.0004 s. After setting up, simulate the fluid domain model through simulation.

DEM Model of Wheat Threshing Mixture

Bags were placed at the grain outlet of the wheat harvester working in the field to collect the mixture threshed by the cleaning device. The proportions of wheat grains and stalks in the threshed mixture were measured to be 90.64% and 9.3%, respectively.

To construct a 3D model of wheat grains, 50 grains were randomly selected from the harvested wheat. Their average dimensions along the three axes were recorded using a vernier caliper, and the average values were calculated. Based on the results, the standard model dimensions for wheat grains were set to 6.76 mm×2.98 mm×2.88 mm. Using the obtained average dimensions of wheat grains, a 3D solid model was created with SOLIDWORKS software. The multi-sphere method was used in EDEM software to densely fill the 3D model, and a comparison between the filled particle model and actual wheat is shown in the figure.



(1) Wheat seeds (2) Discrete meta-model of wheat

Fig. 10 – Comparison Diagram of Wheat Seeds and Wheat Discrete Element Model

Similarly, 50 short stalks were randomly selected from the collected samples. After measuring their average dimensions along the three axes, the standard model dimensions for wheat stalks were determined to be a length of 23.54 mm, an outer diameter of 2.23 mm, and a wall thickness of 0.37 mm.

To ensure that the simulation experiments align with the actual conditions of seed production harvesting, mechanical properties and contact parameters between materials were determined by comprehensively referencing existing discrete element calibration literature for wheat grains and stalk particles, as well as data obtained from previous observations, measurements, and experimental studies. These parameters are shown in Tables 3 and 4.

Table 3

Material mechanical properties parameters			
Material	Poisson ratio	Shear modulus/pa	Density/kg-m ⁻³
Wheat seeds	0.3	2.6	1350
Short stalk	0.4	1	104
Cleaning sieve (Steel plate)	0.3	7800	7800

Table 4

Contact coefficient between materials			
Contact property	Restitution coefficient	Coefficient of static friction	Coefficient of rolling friction
Grain-Grain	0.2	1	0.01
Grain-Stem	0.3	0.5	0.01
Grain-Steel plate	0.45	0.35	0.01
Stem-Steel plate	0.3	0.36	0.01
Stem-Stem	0.22	0.5	0.01

The mass ratio measurement test was carried out on the mixture removed from the cleaning device obtained from the field. The mass ratio of each component of the mixture was 90.64 % of the grain mass and 9.3 % of the residual mass. Combined with the parameters of grain weight, grain and stem density, the number of particles generated in the simulation was calculated to be 4200 wheat grains and 450 wheat short stems, respectively. The particles were generated within 2.0 s.

Screening Simulation Process and Result Analysis

The figure below illustrates the cleaning states of the separation device at different time intervals, where the red spherical particles represent wheat seeds and the blue cylindrical particles represent short stalks.

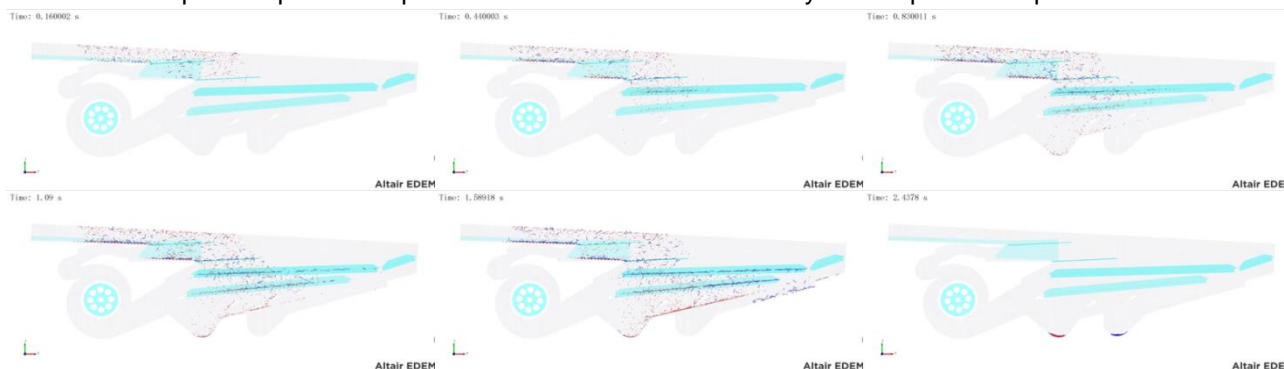


Fig. 11 – Simulation Time Frame Diagram of the Cleaning Chamber

Based on the illustration, it can be observed that at 0.16 seconds, the mixture particles begin to form in the particle generator and randomly fall onto the shaking plate. By 0.44 seconds, the particles come into contact with the cleaning screen and start moving towards the end of the screen due to the combined action of airflow and screening motion. At 0.83 seconds, some particles pass through the screen surface, and the wheat seeds, guided by the baffle plate, fall into the grain collection auger. By 1.09 seconds, a large number of mixture particles move towards the tail under the dual influence of airflow and screening motion, while light impurities are expelled out of the machine through the upper air outlet. At 1.58 seconds, the short stalks and light impurities are steadily discharged through the upper air outlet, and a large number of particles pass through the double-layer vibrating screen, guided by the baffle plates into the grain collection auger and the debris auger, respectively. By 2.4 seconds, the cleaning process is essentially complete; under the synergistic effect of airflow from the fan's dual outlets and screening motion, the vast majority of wheat seeds fall into the grain collection auger, with some entering the debris auger. These seeds, along with the debris, are transported by the auger above the vibrating screen for re-screening, with only a very small number of wheat seeds being expelled from the machine during the airflow and screening movements.

EXPERIMENTAL STUDY AND RESULT ANALYSIS OF WHEAT SEED SEPARATION AND CLEANING PERFORMANCE

Design of Experiments with Multiple Factors

To further investigate the combined effects of multiple factors on the performance of the cleaning device in wheat seed harvesting machines, the significance levels of various factors on the impurity rate and cleaning loss rate indicators are analyzed. This helps to determine the priority and influence order of each experimental factor on the test indicators and to identify the optimal parameter combinations. This analysis provides a theoretical basis for selecting factor levels in subsequent regression experiments. The experiment considers fan speed (X_1), amplitude (X_2), and vibration frequency (X_3) as experimental factors, and impurity rate (Y_1) and loss rate (Y_2) as the indicators of cleaning effectiveness, conducting a three-factor, three-level response surface experiment.

In the preliminary single-factor simulation experiments, impurity rate and loss rate were used as experimental indicators, while fan speed (900-1300 rpm), amplitude (10-50 mm), and vibration frequency (5-15 Hz) were considered as experimental factors. Specifically, when the fan speed was less than 1100 rpm material accumulation occurred, making it difficult for wheat seeds to pass through the sieve, resulting in an increased impurity rate. When the amplitude was less than 20 mm and the vibration frequency was less than 6 Hz, the separation effect between wheat seeds and short stalks was poor, leading to low cleaning efficiency. Conversely, when the amplitude exceeded 40 mm and the vibration frequency was greater than 10 Hz, there was significant fluctuation in the transport state of materials on the sieve surface, causing material splashing and a substantial increase in cleaning loss rate. Based on the analysis results of the single-factor experiments, the levels for fan speed were set at 1100 rpm, 1200 rpm, and 1300 rpm; the levels for cleaning sieve amplitude were set at 20 mm, 30 mm, and 40 mm; and the levels for vibration frequency were set at 6 Hz, 8 Hz, and 10 Hz. The coding table for experimental factor levels is shown in Table 5.

Table 5

Test code table			
Coding Level	Experimental factors		
	Fan speed X ₁ (rpm)	Amplitude X ₂ (mm)	Vibration frequency X ₃ (Hz)
-1	1100	20	6
0	1200	30	8
1	1300	40	10

Results and Analysis of Multi-Factor Experiments

The experimental setup and results are shown in the table. From the response surface experiment results, it can be seen that the range of seed admixture rate in this experiment is 1.15~1.96%, and the range of seed loss rate is 0.64~1.82%.

Table 6

Test design and results					
Experimental coding	Experimental factors			Hybridization rate of seeds Y ₁ /%	Losing seed rate Y ₂ /%
	Fan speed X ₁ (rpm)	Amplitude X ₂ (mm)	Vibration frequency X ₃ (Hz)		
1	1100	20	8	1.89	0.64
2	1300	20	8	1.29	1.02
3	1100	40	8	1.31	1.05
4	1300	40	8	1.17	1.92
5	1100	30	6	1.96	0.68
6	1300	30	6	1.34	1.23
7	1100	30	10	1.28	0.81
8	1300	30	10	1.21	1.74
9	1200	20	6	1.88	0.85
10	1200	40	6	1.29	1.36
11	1200	20	10	1.3	0.89
12	1200	40	10	1.15	1.82
13	1200	30	8	1.23	1.03
14	1200	30	8	1.19	0.99
15	1200	30	8	1.25	0.96
16	1200	30	8	1.27	0.94
17	1200	30	8	1.2	1.01

Perform a second-order multivariate regression fitting based on the simulation test data, and use Design-Expert 13 software to conduct regression analysis on seed admixture rate (Y₁) and seed loss rate (Y₂).

The regression equations for seed admixture rate (Y₁) and seed loss rate (Y₂) are:

$$Y_1 = 1.23 - 0.1788A - 0.18B - 0.1913C + 0.115AB + 0.1375AC + 0.11BC + 0.1148A^2 + 0.0723B^2 + 0.1047C^2 \tag{14}$$

$$Y_2 = 0.986 + 0.3412A + 0.3437B + 0.1425C + 0.1225AB + 0.095AC + 0.1050BC + 0.0283A^2 + 0.1433B^2 + 0.1007C^2 \tag{15}$$

To further analyze the impact of various experimental factors on the test indices, Design-Expert 13 software was used to obtain the response surface, as shown in the figure 12.

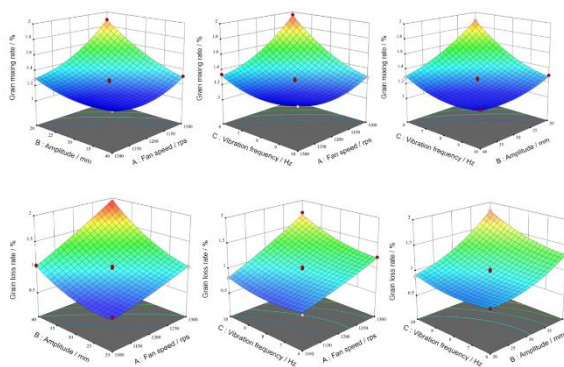


Fig. 12 – The response surface variation relationship of each factor to the test index

Experimental Optimization

In order to optimize the performance of the cleaning device and improve the effectiveness of seed harvesting, the fan speed, amplitude, and vibration frequency were subjected to parameter optimization design with the minimization of admixture rate and loss rate as the optimization objectives. The weight for admixture rate was set to five "+", and the weight for loss rate was set to three "+". The target values for the three factors were set within the optimization range, establishing a parametric mathematical model as follows:

$$\begin{cases} \min Y_1 \\ \min Y_2 \\ s.t. \begin{cases} 1100rps \leq X_1 \leq 1300rps \\ 20mm \leq X_2 \leq 40mm \\ 6Hz \leq X_3 \leq 10Hz \end{cases} \end{cases} \quad (16)$$

Using multi-objective parameter optimization in Design-Expert 13 software to analyze the mathematical model, the results indicate that the optimal operating parameters for the cleaning device are a fan speed (X_1) of 1143 rpm, an amplitude (X_2) of 28 mm, and a vibration frequency (X_3) of 9.4 Hz.

FIELD TEST

Building on the design of the cleaning device, its operating parameters were set according to the simulation test results and applied to the 4LX-1 wheat plot harvester. On June 22, 2024, a field trial was conducted at the Weifang Modern Agricultural Science and Technology Demonstration Park, harvesting the wheat variety "Zhengmai 113" at its optimal harvest time. The calculation formulas for seed admixture rate and seed loss rate are as follows:

$$P_z = \frac{M_z - M_m}{M_z} \times 100\% \quad (17)$$

$$P_s = \frac{M_b}{M_a + M_b} \times 100\% \quad (18)$$

In the formula: P_z represents the seed admixture rate, expressed as a percentage (%); M_z denotes the mass of the mixture in the grain collection auger, in g; M_m is the mass of seeds in the grain collection auger after impurities have been removed, in g; P_s represents the seed loss rate, expressed as a percentage (%); M_a is the harvested wheat seed yield per square meter, in g; M_b is the seed loss per square meter of wheat, in g.

Table 7

Serial number	Field test results	
	Low-loss and high-purity cleaning device	
	Hybridization rate of seeds/%	Losing seed rate/%
1	1.66	0.96
2	1.91	1.12
3	1.27	1.33
4	1.41	1.04
5	1.1	0.91
Mean value	1.47	1.07

The seed admixture rate and seed loss rate were calculated according to the formula, and the results are shown in the table. Under the optimal parameter combination of the optimized cleaning device, the average wheat admixture rate was 1.47%, and the average loss rate was 1.04%.

The operational results were similar to the simulation test results, with all indicators meeting the standards for seed production and harvesting. Therefore, the improved cleaning device is suitable for wheat seed production and harvesting operations.



Fig. 13 – Collection of Threshed Material and Field Test Diagram

CONCLUSIONS

(1) In this paper, a low-loss and high-purity cleaning device suitable for wheat breeding and harvesting operations was designed. The motion model of the sieve body and the material was established. It was determined that the operation effect of the cleaning device was affected by three important factors : fan speed, amplitude and vibration frequency.

(2) The CFD-DEM coupling simulation method was used to analyze the screening process of the separated mixture under the action of the fan, and the optimal structural parameters were obtained by combining the single factor test. The parameter combination was optimized with the minimum seed mixing rate and seed loss rate as the optimization objective, and the field verification test was carried out. The average mixing rate of wheat was 1.47 %, and the average loss rate was 1.04 %. The operation results were similar to the simulation test results, and all indicators met the relevant standards.

ACKNOWLEDGEMENT

The author was supported by the "National Key R&D Program" (2023YFD2000404-2) and "Mount Taishan Industrial Leading Talent Project in Shandong Province" (LJNY201804).

REFERENCES

- [1] Buryanov A., Chervyakov I. (2019). Using combines for cleaning grain crops by non-traditional technologies, *INMATEH – Agricultural Engineering*, 59(3), pp. 27-32.
- [2] Cheli, F., Abdelaziz, A. K. M., Arrigoni, S., Paparazzo, F., & Pezzola, M. (2024). Precision Agriculture Applied to Harvesting Operations through the Exploitation of Numerical Simulation. *Sensors*, 24(4), 1214.
- [3] Delaney, G. W., Cleary, P. W., Hilden, M., & Morrison, R. D. (2012). Testing the validity of the spherical DEM model in simulating real granular screening processes. *Chemical Engineering Science*, 68(1), 215-226.
- [4] Ding, B., Liang, Z., Qi, Y., Ye, Z., & Zhou, J. (2022). Improving Cleaning Performance of Rice Combine Harvesters by DEM–CFD Coupling Technology. *Agriculture*, 12(9), 1457.
- [5] Fu, J., Zhang, M., Cheng, C., Zhao, H., & Ren, L. (2024). Thickness monitoring of threshing mixture on the oscillating plate of corn grain harvester. *Computers and Electronics in Agriculture*, 227, 109485.
- [6] Gao, X., Cui, T., Zhou, Z., Yu, Y., Xu, Y., Zhang, D., & Song, W. (2021). DEM study of particle motion in novel high-speed seed metering device. *Advanced Powder Technology*, 32(5), 1438-1449.
- [7] Hevko R.B., Tkachenko I.G., Rogatynskiy R.M., Synii S.V., Flonts I.V., Pohrishchuk B.V. (2019). Impact of parameters of an after-cleaning conveyor of a root crop harvester on its performance, *INMATEH – Agricultural Engineering*, 59(3), pp. 41-48.
- [8] Ivan Gh., Vlăduț V., Ganea I. (2015). Improving threshing system feeding of conventional cereal harvesting combine, *Proceedings of the 43 International Symposium on Agricultural Engineering "Actual Tasks on Agricultural Engineering"*, pp. 431-440, Opatija – Croatia.
- [9] Krishna, T. P. A., Veeramuthu, D., Maharajan, T., & Soosaimanickam, M. (2023). The era of plant breeding: Conventional breeding to genomics-assisted breeding for crop improvement. *Current Genomics*, 24(1), 24-35.

- [10] Lalghorbani, H., & Jahan, A. (2022). Selection of a wheat harvester according to qualitative and quantitative criteria. *Sustainability*, 14(3), 1313.
- [11] Lenaerts, B., Aertsen, T., Tijsskens, E., De Ketelaere, B., Ramon, H., De Baerdemaeker, J., & Saeys, W. (2014). Simulation of grain–straw separation by Discrete Element Modeling with bendable straw particles. *Computers and Electronics in Agriculture*, 101, 24-33.
- [12] Li, H., Li, Y., Gao, F., Zhao, Z., & Xu, L. (2012). CFD–DEM simulation of material motion in air-and-screen cleaning device. *Computers and Electronics in Agriculture*, 88, 111-119.
- [13] Li, Y., Xu, L., Lv, L., Shi, Y., & Yu, X. (2022). Study on modeling method of a multi-parameter control system for threshing and cleaning devices in the grain combine harvester. *Agriculture*, 12(9), 1483.
- [14] Liang, Z. (2021). Selecting the proper material for a grain loss sensor based on DEM simulation and structure optimization to improve monitoring ability. *Precision Agriculture*, 22(4), 1120-1133.
- [15] Liu, P., Wang, XY., & Jin, CQ. (2022). Bench test and analysis of cleaning parameter optimization of 4 L-2.5 wheat combine harvester. *Applied Sciences*, 12(18), 8932.
- [16] Marin E., Cârdei P., Vlăduț V., Biriș S-Șt., Ungureanu N., Bungescu S.T., Voicea I., Cujbescu D., Găgeanu I., Popa L-D., Isitcioaia S., Matei Gh., Boruz S., Teliban G., Radu C., Kabas O., Caba I., Maciej J. (2023). Research on the influence of the main vibration-generating components in grain harvesters on the operator's comfort, INMATEH – Agricultural Engineering 74 (3), pp. 800-815.
- [17] Mehta, C. R., Chandel, N. S., Jena, P. C., & Jha, A. (2019). Indian agriculture counting on farm mechanization. *Agricultural Mechanization in Asia, Africa and Latin America*, 50(1), 84-89.
- [18] Mircea C., Nenciu F., Vlăduț V., Voicu Gh., Gageanu I., Cujbescu D. - Increasing the performance of cylindrical separators for cereal cleaning, by using an inner helical coil, *INMATEH – Agricultural Engineering*, vol. 62, no. 3 / 2020, pp. 249-258.
- [19] Parihar, D. S., Dogra, B., Narang, M. K., Javed, M., & Singh, D. (2023). Integrated seeding attachment for combine harvesters: a sustainable approach for conservation agriculture. *Environment, Development and Sustainability*, 1-21.
- [20] Safranyik, F., Csizmadia, B. M., Hegedus, A., & Keppler, I. (2019). Optimal oscillation parameters of vibrating screens. *Journal of Mechanical Science and Technology*, 33, 2011-2017.
- [21] Suardi, A., Stefanoni, W., Bergonzoli, S., Latterini, F., Jonsson, N., & Pari, L. (2020). Comparison between two strategies for the collection of wheat residue after mechanical harvesting: Performance and cost analysis. *Sustainability*, 12(12), 4936.
- [22] Török, K., Szentmiklóssy, M., Tremmel-Bede, K., Rakszegi, M., & Tömösközi, S. (2019). Possibilities and barriers in fibre-targeted breeding: Characterisation of arabinoxylans in wheat varieties and their breeding lines. *Journal of Cereal Science*, 86, 117-123.
- [23] Vlăduț N.-V., Biriș S.St., Cârdei P., Găgeanu I., Cujbescu D., Ungureanu N., Popa L.-D., Perișoară L., Matei G., Teliban G.-C. (2022). Contributions to the Mathematical Modeling of the Threshing and Separation Process in An Axial Flow Combine, *Agriculture*, 12(10), 1520.
- [24] Vlăduț N.-V., Ungureanu N., Biriș S.St., Voicea I., Nenciu F., Găgeanu I., Cujbescu D., Popa L.-D., Boruz S., Matei G., Ekielski A., Teliban G.C. (2023). Research on the identification of some optimal threshing și separation regimes in the axial flow apparatus, *Agriculture*, 13(4): 838.
- [25] Wang, L., Chai, X., Huang, J., Hu, J., & Cui, Z. (2024). Efficient and Low-Loss Cleaning Method for Non-Uniform Distribution of Threshed Materials Based on Multi-Wing Curved Combination Air Screen in Computational Fluid Dynamics/Discrete Element Method Simulations. *Agriculture*, 14(6), 895.
- [26] Wang, L., Zhang, S., Gao, Y., Cui, T., Ma, Z., & Wang, B. (2023). Investigation of maize grains penetrating holes on a novel screen based on CFD-DEM simulation. *Powder Technology*, 419, 118332.
- [27] Zhang, C., Geng, D., Xu, H., Li, X., Ming, J., Li, D., & Wang, Q. (2023). Experimental Study on the Influence of Working Parameters of Centrifugal Fan on Airflow Field in Cleaning Room. *Agriculture*, 13(7), 1368.